Out of the Mediterranean? Post-glacial colonization pathways varied among cold-water coral species

Boavida Joana [1, 2, 3, *] , Becheler Ronan [4, 5, 6], Choquet Marvin [4, 7], Frank Norbert [8], Taviani Marco [9, 10, 11], Bourillet Jean-Francois [12], Meistertzheim Anne-leila [13, 14], Grehan Anthony [15], Savini Alessandra [16], Arnaud-Haond Sophie [1, 15]

[1] MARBEC, Institut Français de Recherche pour L'Exploitation de la MerUniv MontpellierCNRSIRD Sète ,France
[2] Aix Marseille UniversitéCNRS/INSUUniversité de ToulonIRDMediterranean Institute of Oceanography (MIO) UM 110 Marseille ,France
[3] Centro de Ciências do MarUniversidade do Algarve Faro, Portugal
[4] Institut Français de Recherche pour L'Exploitation de la MerCentre de BretagneREM/EEPLaboratoire Environnement Profond Bretagne ,France
[5] CNRSUMI 3614 Evolutionary Biology and Ecology of AlgaeSorbonne UniversitéUPMC Univ Paris 6 Roscoff ,France
[6] Station Biologique de Roscoff ,Roscoff Cedex ,France
[7] Faculty of Biosciences and AquacultureNord University Bodø ,Norway
[8] Institute of Environmental PhysicsHeidelberg University Heidelberg ,Germany
[9] Institute of Marine Sciences - National Research Council (ISMAR-CNR) Bologna, Italy
[10] Biology DepartmentWoods Hole Oceanographic Institution Woods Hole Massachusetts, usa
[11] Stazione Zoologica Anton Dohrn Villa Comunale Naples, Italy
[12] Institut Français de Recherche pour L'Exploitation de la MerPhysical Resources and Sea Floor Ecosystems Department Brest ,France
[13] CNRSSorbonne UniversitésLaboratoire d'Ecogéochimie des Environnements Benthiques (LECOB) Banyuls-sur-Mer ,France
[14] CNRSSorbonne UniversitésLaboratoire d'Océanographie Microbienne (LOMIC) Banyuls-sur-Mer ,France
[15] Department of Earth & Ocean SciencesNUI Galway Galway ,Ireland
[16] Department of Earth and Environmental SciencesUniversità degli Studi di Milano-Bicocca Milano ,Italy

* Corresponding author : Joana Boavida, email address : joanarboavida@gmail.com

Abstract :

Aim

To infer cold-water corals' (CWC) post-glacial phylogeography and assess the role of Mediterranean Sea glacial refugia as origins for the recolonization of the northeastern Atlantic Ocean.

Location

Northeastern Atlantic Ocean and Mediterranean Sea.

Taxon

Lophelia pertusa, Madrepora oculata.

Methods

We sampled CWC using remotely operated vehicles and one sediment core for coral and sediment dating. We characterized spatial genetic patterns (microsatellites and a nuclear gene fragment) using networks, clustering and measures of genetic differentiation.

Results

Inferences from microsatellite and sequence data were congruent, and showed a contrast between the two CWC species. Populations of L. pertusa present a dominant pioneer haplotype, local haplotype radiations and a majority of endemic variation in lower latitudes. Madrepora oculata populations are differentiated across the northeastern Atlantic and genetic lineages are poorly admixed even among neighbouring sites.

Conclusions

Our study shows contrasting post-glacial colonization pathways for two key habitat-forming species in the deep sea. The CWC L. pertusa has likely undertaken a long-range (post-glacial) recolonization of the northeastern Atlantic directly from refugia located along southern Europe (Mediterranean Sea or Gulf of Cadiz). In contrast, the stronger genetic differentiation of M. oculata populations mirrors the effects of long-term isolation in multiple refugia. We suggest that the distinct and genetically divergent, refugial populations initiated the post-glacial recolonization of the northeastern Atlantic margins, leading to a secondary contact in the northern range and reaching higher latitudes much later, in the late Holocene. This study highlights the need to disentangle the influences of present-day dispersal and evolutionary processes on the distribution of genetic polymorphisms, to unravel the influence of past and future environmental changes on the connectivity of cosmopolitan deep-sea ecosystems associated with CWC.

v. Acknowledgements

Introduction

Cold-water coral (CWC) reefs are among the most charismatic marine ecosystems in the deep ocean (>200 m), supporting abundant and diverse biomass (Milligan et al., 2016). Deep-reef habitats rely upon the frame-building capability of several coral species, notably *Lophelia pertusa* (Linnaeus, 1758) and *Madrepora oculata* (Linnaeus, 1758). These two species intermingle and anastomose in reefs in the northeastern Atlantic Ocean (NE Atlantic; Arnaud-Haond et al., 2017). However, constantly rising anthropogenic pressures in the deep-sea, such as fishery exploitation (Pusceddu et al., 2014), oil and gas exploitation (Cordes et al., 2016) and deep-sea mining (Wedding et al., 2015), threaten vulnerable CWC. Protection of key deep-sea ecosystems is, therefore, an urgent priority, particularly in the face of global change, and strategic Marine Protected Areas thoroughly assessed for their genetic connectivity, need to be established. Nonetheless, obtaining sufficient specimens and applying statistically robust sampling designs in genetic studies in the deep-sea remain challenging (Becheler et al., 2017). While CWC connectivity has been assessed along the North Atlantic Ocean at local and regional scales (LeGoff-Vitry et al., 2004; Morrison et al., 2011; Dahl et al., 2012; Becheler et al., 2017), effective conservation warrants information at the NE Atlantic basin scale (Fenberg et al., 2012). Spatial distribution analyses of genetic diversity can be used to detect connectivity pathways across reefs, and to define key areas for the conservation of biodiversity.

Similarly, the present-day geographic distribution of many terrestrial and marine species and their genetic diversity are influenced by environmental gradients, contemporary dispersal and recent climatic events, notably the Last Glacial Maximum (LGM, 26 - 19 ka; Hewitt, 1996, 1999, 2004; Petit et al., 2003; Maggs et al., 2008; Clark, 2009). Repeated Pleistocene glaciations are known to impact deep-sea ecosystems (Bouchet & Taviani, 1992; Sabelli & Taviani, 2014; Vertino et al., 2014). However, their impact on CWC in particular remains understudied. The responses of deep-sea species may not be similar to those of coastal species, because biological assemblages, environmental gradients and dispersal patterns are fundamentally different among ecosystems and geographical areas (Kousteni et al., 2015; Shum et al., 2015).

The biogeographic connectivity between Mediterranean and NE Atlantic CWC during and after Pleistocene (ca. 2.7 Ma to 12 ka) glacial events can partially be inferred from paleo-records (Supplementary Paleo-history in Appendix S1). While CWC have maintained a

118 continuous presence in the Mediterranean Sea since at least the early Pleistocene (Vertino et
119 al., 2014), in the NE Atlantic CWC presence may have been more affected by changes in
120 climate, with a consequent local demise during the LGM (Frank et al., 2011). Notably, the last
121 cold oscillation, during the Younger Dryas (12.9-11.7 ka), represented a favourable period for
122 CWC reef growth in the western Mediterranean Sea, as well as in adjacent Atlantic regions in
123 the Gulf of Cadiz and African margins (Schröder-Ritzrau et al., 2005; McCulloch et al., 2010;
124 Taviani et al., 2011). In contrast, growth episodes of CWC in the NE Atlantic have been
125 restricted to warm climate stages and coral fossils are absent from strata corresponding to
126 glacial episodes (Frank et al., 2009). Radiometric dating shows that NE Atlantic CWC are
127 younger than those from the Mediterranean Sea, with ages estimated to be post-LGM (under
128 12,000 years; Freiwald & Roberts, 2005; Schröder-Ritzrau et al., 2005), producing an NE
129 Atlantic CWC age gradient from south to north (summarized in Fig. 1). Given the persistent
130 occurrence of CWC, it has been argued that the Mediterranean basin may have acted as a
131 CWC glacial refugium during range contractions in the North Atlantic Ocean during
132 Pleistocene glaciations (De Mol et al., 2002; Henry et al., 2014). This refugium may have
133 constituted the source for the Atlantic northward recolonisation of CWC at the end of the
134 LGM by larvae, which were transported with intense flows of Mediterranean Outflow Water
135 (MOW) beginning in 50 ka (Fig. 1; Voelker et al., 2006; Stumpf et al., 2010).

136 The sympatric paleo-coral occurrence of *L. pertusa* and *M. oculata* suggests a common
137 history of these species in terms of range contraction and expansion. This common response
138 to past environmental change may not hold true in light of recent studies (Lartaud et al.,
139 2014, 2017) pointing to physiological differences between both species, particularly in terms
140 of optimal growth temperatures. The two CWC may demonstrate dissimilar ecological
141 strategies. *Lophelia pertusa* presents potential for widespread larval dispersal (Strömberg
142 and Larsson, 2017), high fecundity (Waller & Tyler, 2005) and variable microbiome
143 compositions (Meistertzheim et al., 2016). The reproductive strategy of *M. oculata* is different
144 from that of *L. pertusa*, with much lower fecundity (Waller & Tyler, 2005) and a resilient
145 microbiome (Meistertzheim et al., 2016; and unknown larval characteristics). Although
146 reduced genetic connectivity has been demonstrated for *L. pertusa* at an inter-basin scale,
147 along with moderate to high gene flow within regions (Morrison et al., 2011; Dahl et al., 2012;
148 Flot et al., 2013), the extent of CWC connectivity along the European margins and the role
149 that extant populations had in the past remain to be tested. Here, we investigate the
150 population genetic diversity and structure of *L. pertusa* and *M. oculata* along the deep
151 margins of the NE Atlantic using nuclear data (microsatellites and sequences). We discuss
152 how past environmental variations related to the LGM may have affected the genetic diversity
153 and structure of the two CWC species across this wide geographic region. We hypothesise
154 that distinct ecological requirements in the deep-sea influenced population structure and the
155 distribution of genetic diversity within species. In particular, we expected that *L. pertusa*
156 would present low levels of population differentiation across the NE Atlantic margins,
157 consistent with a post-LGM northward expansion from southern refugia and maintained by
158 present-day connectivity. We expected *M. oculata* to present stronger population
159 differentiation than *L pertusa*, consistent with the lower fecundity of *M. oculata*. To these
160 aims, we examined the genetic structure and diversity of *L. pertusa* and *M. oculata* within and
161 among the principal biogeographic provinces of the NE Atlantic and the Mediterranean Sea
162 where CWC are known to occur.

2. Materials and methods

2.1 Field collections

Two hundred and seventy samples of *Lophelia pertusa* and 260 samples of
Madrepora oculata were collected during the period of 2007–2012 from six regions between
250 and 1,170 m depth: the eastern Mediterranean basin (Ionian Sea, south-eastern Adriatic
Sea), western Mediterranean basin (Gulf of Lions); Mid-Atlantic region (Azores), Bay of
Biscay, SE Rockall Bank (off western Ireland), and the High latitudes (Iceland) (Fig. 1; Table
S1 in Appendix S1). In one canyon of the Bay of Biscay, Petite Sole, two sample collections
were conducted at different sections of the canyon. Samples were stored in 96% ethanol and
frozen at -20 or -80°C prior to DNA extraction. *Lophelia pertusa* DNA was extracted aboard
using the Fast DNA®SPIN for soil kit, according to the manufacturer's protocol (MP
Biomedicals, France); for *M. oculata* we used cetyl trimethyl ammonium bromide for DNA
extraction (Doyle & Doyle, 1988). Sampling permits for the Bay of Biscay, Rockall bank and
Iceland were obtained for the entire cruise by the fleet manager (IFREMER; No 347/11;
NV/USEN/No 3278/2012); in the Mediterranean Sea sampling was conducted in compliance
with all relevant regulations for national and international waters; the Azores samples were
collected as fishing by-catch without the need for permits.

2.2 Core collection and dating

Within the Guilvinec Canyon (Bay of Biscay), a 1.2 m-length sediment core (BBCO-CS01)
was collected (N46°56,045'; W005°21,642') at 815 m-depth. The core was representative of
the superficial layers of the Armorican margin. The skeleton remains of corals were dated
using the U/Th method at the Institute for Environmental Physics at Heidelberg University
(Schröder-Ritzrau et al., 2003). Foraminifera from nearby sediments were ^{14}C-dated. Corals
and foraminifera were subsequently calibrated to absolute ages using Intcal13 (Reimer et al.,
2013).

2.3 DNA amplification and sequencing

The internal transcribed spacer (ITS) ribosomal sequence was amplified using primers
developed by Diekmann et al. (2001). ITS sequences (262 samples of *L. pertusa*
1130 base pair, bp, 200 samples of *M. oculata* 1124 bp) were proofread and aligned using
Geneious v6.1 (Kearse et al., 2012). Nine *L. pertusa* (Morrison et al., 2008; Becheler et al.,
2017) and six *M. oculata* microsatellite markers were amplified following Becheler et al.
(2017). Products were scored using Geneious v5.6.4. One *L. pertusa* locus was discarded
due to the high frequency of null alleles (>30%). Clones were removed from each dataset
(ITS and microsatellites). Statistical power was assessed for the two coral species
(Supplementary Methods S2 in Appendix S1). Only sites with five or more samples were kept
for analyses.

2.4 Phylogeographic patterns and genetic diversity

Population genetic differentiation for ITS sequences was assessed with the pairwise
haplotype F_{ST} statistic (Weir & Cockerham, 1984) in Arlequin v3 (Excoffier et al., 2005). The
distribution of genetic variability within and among groups was estimated with analysis of
molecular variance (AMOVA) in Arlequin on four groups for *L. pertusa*, and on five groups
for *M. oculata* (1. Mediterranean, 2. Bay of Biscay, 3. SE Rockall Bank and 4. High Latitudes,
and 5. Mid-Atlantic). Population genetic diversity was estimated with i. the number of distinct
and private haplotypes, ii. number of polymorphic sites, iii. haplotypic diversity (Nei, 1987),

207 and iv. the mean number of pairwise differences (Tajima, 1983). Haplotype relationships
208 were visualized with statistical parsimony networks on TCS v1.21 (Clement et al., 2000)

209 Microsatellite genetic diversity and structure were estimated with GENETIX v4.05 (Belkhir K.,
210 Borsa P., Chikhi L., 2004). The mean number of alleles per locus was standardized to the
211 lowest number of samples collected; estimates of observed (H_O) and unbiased (H_E)
212 multilocus heterozygosity (Nei, 1978), the F_{IS}-statistic and its significance (tested with
213 1000 permutations), and linkage disequilibrium, which was assessed through the index $\check{r}_d$
214 with MULTILOCUS v1.3 (http://www.bio.ic.ac.uk/evolve/software/multilocus/), were calculated.
215 Genetic structure (pairwise F_{ST}) was estimated with θ (Weir & Cockerham, 1984). Inference
216 of spatial population structure with Bayesian clustering was performed with TESS v2.3
217 (François et al., 2006; Chen et al., 2007) via the '*tess3r*' R package (Caye et al., 2016; The R
218 Foundation for Statistical Computing, 2018).

219 We used discriminant analysis of principle components (DAPC; Jombart et al., 2010)
220 implemented in the R package '*adegenet'* (Jombart, 2008), to determine whether the
221 genotypes of *L. pertusa* and *M. oculata* were distinct between different sampling sites. We
222 used k-means clustering (k=2 to maximum number of sampling sites) with the Bayesian
223 information criterion (BIC) to identify the optimal number of genetic clusters describing the
224 data. The α-score optimisation procedure was used to identify the optimal number of
225 principal components (PCs) to retain (retaining too many PCs can lead to overfitting the
226 discriminant functions). α-score optimisation showed that approximately 25 PCs needed to
227 be retained for *M. oculata* (>69.3% of the total variance), and 60 PCs needed to be retained
228 for *L. pertusa* (28.9%). Next, we used DAPC to derive membership probabilities for each
229 individual in each of the groups using location priors (see Supplementary methods S2 in
230 Appendix S1).

2.5 Demographic inferences

232 Historical fluctuations in population size for each sampled site were detected using Fu's Fs
233 (Fu, 1996) and Tajima's D (Tajima, 1989) on ITS data from *L. pertusa* and *M. oculata*.
234 Departures from mutation-drift equilibrium were tested with ARLEQUIN under the null
235 hypothesis of no significant change in effective population size. A negative value significantly
236 different from constant population size was interpreted as a signature of population
237 expansion; the significance of Fs and D values was determined by randomization.

238 The evolutionary and demographic histories of NE Atlantic and Mediterranean CWC
239 (*L. pertusa* and *M. oculata*) were further reconstructed using approximate Bayesian
240 computations (ABC) implemented in DIYABC v2.1.0 (Cornuet et al., 2014). We used
241 microsatellite and ITS sequence data for *M. oculata* and microsatellite data only for
242 *L. pertusa*. *Lophelia pertusa* populations were grouped according to microsatellite Bayesian
243 clustering (cluster 1 - Eastern Mediterranean, cluster 2 - Western Mediterranean, cluster 3 -
244 Bay of Biscay and High latitudes, cluster 4 - SE Rockall bank), and for *M. oculata*, we used
245 the geography-based population grouping (models of *L. pertusa* using geography-based
246 population groups along with further details are found in Appendix S1). We compared
247 competing scenarios in order to identify the patterns of post-LGM CWC range expansion
248 along the NE Atlantic margins. Scenarios 1, 2 and 4 determined the pattern of colonisation of
249 the northern edge of the NE Atlantic range, comparing models of stepping-stone colonization
250 from the Mediterranean Sea to the Bay of Biscay and then further north (Scenario 1 -
251 stepwise range expansion), and models of admixture between the Bay of Biscay, High
252 latitudes and West Mediterranean to produce the SE Rockall bank population (Scenario 2,
253 *L. pertusa*), between the High latitudes and SE Rockall bank to produce the Mid-Atlantic

254   population (Scenario 2, *M. oculata*), between the Bay of Biscay and SE Rockall bank to
255   produce the Mid-Atlantic population (Scenario 4, *M. oculata*), and between the Mediterranean
256   Sea and the Bay of Biscay to produce the Mid-Atlantic population (Scenario 5, *M. oculata*).
257   Scenario 3 examined the demographic history of the NE Atlantic and Mediterranean
258   populations with changes in population size since colonisation. We compared a null model of
259   no change in population size (Scenarios 1 and 2) to a model of a short bottleneck (10
260   generations) during colonisation followed by population expansion (Scenario 3). In this
261   scenario, at each split, there is an initial reduction in the size of the newly formed population
262   because the expansion is assumed to start with few immigrants. For *L. pertusa*, we used the
263   geologically inferred time of SE Rockall bank colonisation (approx. 9 ka; Frank et al., 2009) to
264   calibrate divergence times (mode and 95% confidence interval) from the estimated ABC
265   number of generations; we then assumed the same generation time (est. approx. 3 years) for
266   *M. oculata*.

267   We generated 3 to 5×10^6 simulations for each scenario tested using the combined
268   microsatellite and ITS datasets for *M. oculata* and the microsatellite dataset for *L. pertusa*
269   (Supplementary methods S2 in Appendix S1) to produce a set of pseudo-observed datasets
270   (PODs). Effective population sizes and parameters for the generalized stepwise mutation
271   and Kimura two-parameter models were set to default values, while the time of population
272   divergence (in generations) was defined as uniform within post-LGM periods (for model
273   parameters, see Supplementary Methods S2 in Appendix S1). The posterior probability of
274   each scenario was inferred with a logistic regression performed on the 1% of PODs closest
275   to the empirical data. We empirically evaluated the power of the model to discriminate among
276   scenarios using a Monte Carlo estimation of false allocation rates (type 1 and 2 errors)
277   resulting from ABC posterior probability-based model selection.

278   Supplementary Methods can be found in the Appendix S1.

279   ## 3. Results

280   ### 3.1 Core collection and dating

281   Fossils of *Lophelia pertusa* and *Madrepora oculata* were found in the gravity core. The dating
282   of CWC remains revealed ages ranging from present to 6,959 ± 169 years (U/Th corrected
283   age).

284   ### 3.2 Phylogeographic patterns and genetic diversity

285   TESS analyses showed *Lophelia pertusa* had four genetically distinct groups: the eastern
286   and the western Mediterranean Sea, the SE Rockall bank and the remaining NE Atlantic
287   populations (Bay of Biscay and High latitudes; Fig. 2a right). Within *L. pertusa*, the
288   Mediterranean genetic ancestry, in particular the West Mediterranean ancestry (blue), had
289   low proportions across all NE Atlantic sites. The green genetic ancestry was maximized in
290   the Bay of Biscay and High latitude populations, while the grey genetic ancestry (found in the
291   Bay of Biscay and High latitudes sites) was maximized in the SE Rockall bank population.
292   The grey ancestry component was present in high proportions in the High latitude
293   populations, particularly in Hafadsjup (Iceland, HAF), where it comprised over half of the
294   *L. pertusa* ancestry.

295   The genetic differentiation estimated through AMOVA and pairwise F_{ST} (Table S4.1 and S5.1
296   in Appendix S1) was strong between the East and West Mediterranean populations and
297   weak across the NE Atlantic samples, with almost no values significantly different from zero.
298   The SE Rockall bank population was differentiated from over half of the Bay of Biscay
299   locations but not from the High latitude populations (Table S5.1 in Appendix S1).

300 Clustering performed with TESS showed that *M. oculata* was also structured in four genetic
301 clusters but with a different organisation (Fig. 2a). The Mediterranean Sea and the High
302 Latitudes formed two distinct clusters (displayed in red and grey in Fig. 2a left). The next two
303 clusters were less geographically coherent: the Bay of Biscay genetic ancestry (blue; third
304 cluster) was nearly absent from the Lampaul canyon population, as well as from the SE
305 Rockall bank and Mid-Atlantic populations (which together form the fourth cluster). *M. oculata*
306 populations from the Bay of Biscay harboured a strong Mediterranean genetic component
307 (red) maximized in the populations of the northern Bay of Biscay canyons (Morgat, Crozon
308 and Petite Sole) but absent from most individuals in the Mid-Atlantic, Lampaul canyon (in the
309 Bay of Biscay) and SE Rockall bank populations. The NE Atlantic genetic ancestry (green)
310 was well represented in all NE Atlantic populations and in smaller proportions in some
311 Mediterranean individuals. High latitude genetic ancestry (grey) was found in high
312 proportions in the SE Rockall and Mid-Atlantic populations.

313 The mean pairwise F_{ST} between regions was high for *M. oculata*, with a value up to 0.5
314 between the eastern Mediterranean Sea and High Latitudes, but not significantly different
315 from zero between the eastern and western Mediterranean Sea populations, while nearly all
316 pairwise F_{ST} values were significantly different from zero (Table S4.2 and S5.2 in appendix).
317 A lack of population differentiation was observed between two Bay of Biscay canyons (CRZ-
318 LMP), within one canyon (PS1-PS2), between High latitude locations, and between SE
319 Rockall bank and its closest High latitude site, Londsjup (Table S5.2 in Appendix S1). The
320 regional F_{ST} was significantly different from zero for all pairwise comparisons for the two coral
321 species: Mediterranean Sea, Mid-Atlantic, Bay of Biscay, SE Rockall bank and High
322 latitudes. The lowest regional F_{ST} for *M. oculata* was between the High latitude and SE
323 Rockall bank populations (0.051), while that for *L. pertusa* was between the High latitude and
324 Bay of Biscay populations (0.004).

325 The genetic affinities of the sampled individual corals were projected onto principal
326 components (DAPC). For *L. pertusa*, as expected considering the clustering and F_{ST} results,
327 the first axis separates the Mediterranean and NE Atlantic populations. Within each group,
328 genetic variability is spread across the second axis, with the eastern Mediterranean samples
329 at one end and the western Mediterranean samples at the other end; this separation is also
330 clearly visible in the group membership probabilities (in the bottom of Fig. 3b). The NE
331 Atlantic genetic group along PC2 spans samples from the Bay of Biscay to the High latitudes,
332 including the SE Rockall bank (Fig. 3b). For *M. oculata* genetic affinities show a cline on the
333 first axis, separating samples from the lower (Mediterranean) to the higher latitudes. The
334 gradient is visible in the group membership proportions shown in the bottom of Fig. 3a,
335 particularly along the Bay of Biscay canyons and along SE Rockall-High latitude populations.

336 The gene diversity and the average number of alleles per locus for *L. pertusa* and *M. oculata*
337 samples were high and moderate, respectively (*L. pertusa* H_E 0.90 +/- 0.08, and 30.4 alleles
338 per locus; *M. oculata* H_E 0.53 +/- 0.23 and 12.3 alleles per locus; Tables 1 and 2). Regionally,
339 the average allelic richness was higher at intermediate latitudes for both species
340 (Mediterranean: 7 for *L. pertusa* and 3 for *M. oculata*, Bay of Biscay: 16 and 5, SE Rockall
341 Bank: 15 and 6, and High Latitudes: 12 and 4, in the Mid-Atlantic where only *M. oculata* was
342 sampled: 3). Private alleles were present in all sampled *L. pertusa* sites, but were rarely
343 present in *M. oculata* populations. *Madrepora oculata* presented higher private allelic
344 richness in the Mediterranean basin (2-4). An excess of homozygotes was observed in all
345 *L. pertusa* populations and in half of the *M. oculata* sites, particularly along the NE Atlantic
346 populations.

347 The patterns of genetic structure inferred with ITS were generally concordant with those of
348 microsatellites. Based on statistical parsimony, a haplotype network was constructed for

349   *L. pertusa*, with one main ITS lineage inferred as the most likely ancestral haplotype (from a
350   total of 39 haplotypes), which possibly radiated from lower to higher latitudes (>60% of
351   samples), and many rare haplotypes (over 20 unique). The ancestral haplotype was nearly
352   absent from SE Rockall bank *L. pertusa*, supporting the Bayesian clustering, where High
353   latitude and Bay of Biscay samples shared a genetic ancestry (green) almost absent from SE
354   Rockall bank samples. Two other well-represented haplotypes were restricted to i) the Bay of
355   Biscay, High Latitudes and Mediterranean Sea, and ii) mostly the SE Rockall Bank; with a
356   few Bay of Biscay samples (Fig. 2b), supporting the Rockall bank genetic ancestry (grey) as
357   distinct from relatively close populations (Bay of Biscay and High latitudes). The Atlantic sites
358   harboured the majority of sequence variation. The Bay of Biscay had the highest number of
359   haplotypes (24), with 12 unique to this region, but the highest haplotype diversity (H=0.7)
360   was found in the West Mediterranean Sea (Table 3). Ten haplotypes were observed in the
361   Mediterranean Sea, with two unique to the western Mediterranean. Iceland, regardless of its
362   high latitude and recent CWC fossil ages (8.3 Ka, Fig. 1), harboured the second highest
363   number of *L. pertusa* haplotypes (14; Table S6 in Appendix S1), with two haplotypes
364   exclusive to its CWC reefs. *L. pertusa* haplotypes were not particularly clustered, and, except
365   for the inferred ancestral haplotype, most haplotypes were found in moderate to low
366   frequencies at each site (Table S8 in Appendix S1). There were no *L. pertusa* region-specific
367   haplotypes in the Bay of Biscay or the West Mediterranean Sea.

368   There was some phylogeographic clustering for the *M. oculata* haplotype network, with one
369   lineage dominant in the High latitudes and SE Rockall bank, modestly present in distant
370   southern geographic locations (e.g., one sample from the Mediterranean Sea), and absent
371   from the Bay of Biscay. A quarter of all haplotypes were shared across distant geographic
372   regions (i.e., High Latitudes and Mediterranean Sea). Haplotypes found in Mid-Atlantic
373   *M. oculata* were also found in all other regions (one haplotype) or were restricted to the Bay
374   of Biscay and SE Rockall bank (two haplotypes), with one haplotype unique to the Mid-
375   Atlantic site. Private (unique) haplotypes were observed in all regions where *M. oculata* was
376   sampled but not at all sites. Seven haplotypes were well represented, and there was no
377   obvious sign of haplotype radiation (Fig. 2b). Similar to *L. pertusa*, the majority of ITS
378   sequence variation for *M. oculata* occurred in Atlantic sites. The Bay of Biscay and SE
379   Rockall bank presented the highest number of haplotypes (15 and 11, respectively) and the
380   only region-specific haplotype (Table S8 in Appendix S1). Nonetheless, the highest
381   haplotype diversity (H=0.9) was observed in *M. oculata* from the Mid-Atlantic.

382   The populations of *L. pertusa* in the NE Atlantic were slightly differentiated, while within the
383   Bay of Biscay, the genetic structure was weak for *M. oculata* (nearly all pairwise F_{ST} not
384   significantly different from zero; Table S4 in Appendix S1). *Madrepora oculata* showed a
385   regional pattern of population genetic structure concordant with microsatellite analyses (high
386   F_{ST} between populations from distinct regions). Overall, 5% of *L. pertusa* and nearly 40% of
387   *M. oculata* genetic variation occurred among regions (AMOVA; Table S7 in Appendix S1).

388   Haplotypic and molecular diversities varied among locations (Tables 3 and 4). For *L. pertusa*,
389   haplotypic diversity was high (up to 0.6 in the NE Atlantic and up to 0.7 in the Mediterranean
390   Sea) due to haplotype radiations. Haplotypic diversity was also high in *M. oculata* populations
391   (0.3-0.7 in High Latitudes, 0.9 in the Mid-Atlantic site, where there were four haplotypes for
392   five individuals). A comparable pattern of variation of molecular diversity is observed for both
393   species. Nucleotide diversity was lower at the NE Atlantic sites than at the Mediterranean
394   Sea sites for *L. pertusa*. For *M. oculata,* nucleotide diversity was highest in the West
395   Mediterranean and Mid-Atlantic populations.

396   ### 3.3. Demographic inferences

397   The tests of conformity to selective neutrality suggest different demographic histories for
398   *L. pertusa* and *M. oculata*. The Mediterranean populations of *L. pertusa* did not significantly
399   depart from mutation-drift equilibrium (Table 3), while most populations in the Bay of Biscay
400   showed negative Fs and Tajima D values significantly departing from mutation-drift
401   equilibrium. This result is consistent with the network and indicates a recent demographic
402   expansion of the Atlantic populations. All Fs values and most Tajima D values were
403   nonsignificant for *M. oculata*; only two *M. oculata* sites showed Tajima D values significantly
404   departing from constant effective population size, indicating a demographic expansion: one
405   site in the East Mediterranean and one site in the Bay of Biscay (Crozon canyon; Tables 3
406   and 4).

407   Model-based inference pointed to an ancient (up to 30 ka; Table S2 in Appendix S1)
408   divergence of the East and West Mediterranean Sea *L. pertusa* populations, as observed
409   with DAPC. The West Mediterranean population was identified as the source from which all
410   other NE Atlantic populations emerged, either directly (Bay of Biscay and High latitudes;
411   approx. 21 ka) or through admixture (SE Rockall bank; much later at 9 ka), in line with the
412   Bayesian clustering, where the West Mediterranean ancestry (blue) is found throughout the
413   Atlantic sites, and with the ITS network, where most Mediterranean haplotypes are shared
414   with Bay of Biscay corals. The shared SE Rockall genetic ancestry (grey) between the Bay of
415   Biscay and the High latitude populations identified with Bayesian clustering agrees with the
416   admixed origin for the SE Rockall *L. pertusa* found with ABC. The Mediterranean population
417   size estimates (N=2,500 to 7,000) were much smaller than the NE Atlantic size estimates
418   (N=70,000-85,000). The Bay of Biscay demographic expansion scenario with admixture was
419   supported with a high probability relative to the approximately 0.2 support for scenarios of
420   stepping-stone colonisation and changes in population size (Figs. S3-S4 in Appendix S1).
421   The scenario choice confidence was high, with low error rates (posterior predictive error =
422   0.29). Post-LGM range colonisation followed a long-range model of northern range
423   colonisation, whereby the Bay of Biscay and High latitudes were colonised directly from the
424   West Mediterranean Sea populations, while at a later stage the SE Rockall bank was
425   colonised from admixture between Bay of Biscay, High latitude and West Mediterranean
426   populations (Fig. 1 bottom inset).

427   ABC analyses indicated that the Mediterranean Sea *M. oculata* populations were the main
428   source population (N=8,600) from which all other NE Atlantic populations emerged. The
429   Mediterranean source population scenario, with colonisation of the Atlantic margins via the
430   Bay of Biscay agrees with Bayesian clustering, where the Mediterranean genetic ancestry
431   (red) is found in moderate proportions in the Bay of Biscay populations and is absent from
432   the Mid-Atlantic and SE Rockall populations. The scenario of a Mediterranean source
433   population with colonisation of the NE Atlantic and admixture was supported with high
434   probability (0.9) relative to the low support for the scenarios of changes in population size or
435   competing admixture (Figs. S3-S4 in Appendix S1). The scenario choice confidence was
436   high, with low error rates (0.30). Post-LGM range colonisation along the European margins
437   followed a stepping-stone model of northern range colonisation, whereby the Bay of Biscay
438   was colonised directly from Mediterranean Sea populations (22 ka), while the Bay of Biscay
439   *M. oculata* later colonised the SE Rockall bank (7 ka). The SE Rockall bank populations then
440   originated other NE Atlantic *M. oculata* populations. This occurred either through admixture
441   with the Bay of Biscay (Mid-Atlantic) only approximately 2 ka or directly (High latitudes) much
442   more recently (0.3 ka; Fig. 1 top inset). The genetic footprint of those events can be seen in
443   the main haplotype shared between High latitudes and SE Rockall corals but absent from
444   Bay of Biscay corals, by a haplotype restricted to the Bay of Biscay, SE Rockall bank and
445   Mid-Atlantic (haplotype V in Figure S6 Appendix S1), and by the position of Mid-Atlantic
446   samples in the DAPC between SE Rockall and Biscay samples.

Discussion

Although the deep-sea is considered as relatively environmentally stable over time, there is evidence that CWC have undergone demographic changes similar to those experienced by their coastal water counterparts (Wilson & Eigenmann Veraguth, 2010; Sabelli & Taviani, 2014; Vertino et al., 2014; Quattrini et al., 2015). Here, we focused on the LGM and explored two scenarios that could explain the observed patterns of genetic diversity and structure for *L. pertusa* and *M. oculata*, respectively:

i) Before the LGM (to approximately 50 ka, which is the oldest period represented by existing data), NE Atlantic populations were absent from the current northern range of their modern distribution, and present-day patterns of genetic variation were caused by expansion northwards, most likely originated from the West Mediterranean Sea and/or adjacent NW coast of Africa and a later Mediterranean-NE Atlantic admixture;

ii) Before the LGM, NE Atlantic populations were absent from the current northern range of their modern distribution and present-day patterns of genetic variation were caused by "stepping-stone" northwards colonisation with modest demographic expansions and by a much later admixture between NE Atlantic populations with possible contributions from other unsampled populations.

Scenario i)

Geological studies report the absence of deep CWC reef growth in the NE Atlantic during glaciations of the Late Pleistocene (approx. 126 - 12 ka; with the Last Glacial Maximum approx. 26.5-19 ka; Clark et al., 2009; Frank et al., 2009). In contrast, between 50-12 ka, *L. pertusa* reefs flourished in the Mediterranean Sea (Supplementary Paleo-History in Appendix S1). The Mediterranean Outflow Water (MOW 800-1300 m depth; Price et al., 1993) volumes in this period were smaller than those at present (Rogerson et al., 2004) but concentrated in channels with high local flow (Zahn et al., 1997). In the Gulf of Cadiz and on the Moroccan shelf, reef growth was estimated to have started at approximately 40-50 ka (Fig. 1), when glacial conditions were particularly favourable for coral growth, unlike in the NE Atlantic (Schröder-Ritzrau et al., 2005; Eisele et al., 2011; Ramos et al., 2017; Weinberg et al., 2018). The rapid increase in post-glacial Atlantic Meridional Overturning Circulation resulted in increased transport of suspended particles and is speculated to have boosted the expansion of *L. pertusa* from these southern locations (Mediterranean Sea and/or adjacent NW coast of Africa) into the NE Atlantic (Eisele et al., 2011; Fink et al., 2013; Henry et al., 2014).

According to geological analysis, continuous and vertical growth of CWC reefs occurred in the Bay of Biscay area during at least the past 7,000 years. Genetic evidence of recent *L. pertusa* demographic expansions in the Bay of Biscay, at the end of the LGM (approx. 21 ka) is substantiated by internal transcribed spacer sequences with haplotype network and conformity tests and attributed to a founder event, i.e., a dominant haplotype found in all regions (from the Mediterranean Sea to the High Latitudes). Such a demographic expansion would have produced satellite haplotypes with a low genetic distance, as observed in *L. pertusa*. The vast nearly panmictic ensemble occurring along the NE Atlantic indicates a recent common history for Atlantic *L. pertusa* reefs. This is supported by studies of reproduction and larval development that indicate that *L. pertusa* larvae have a long pelagic larval duration, suggesting a high dispersal potential (Waller & Tyler, 2005; Larsson et al., 2014; Strömberg & Larsson, 2017). Larvae of *L. pertusa* maintained in aquaria have been observed swimming towards the surface, yet it remains unknown whether they are neutrally buoyant and remain at spawning depth in their natural environment, i.e., at the depth of the North Atlantic currents shown in Fig. 1. Larval dispersal trajectories may track specific water

495 masses (Dullo et al., 2008) occurring at intermediate depths with potential settling sites. Such
496 a high larval dispersal ability may have favoured large-scale expansion, explaining widely
497 shared genetic ancestry, such as that between *L. pertusa* in the Bay of Biscay and High
498 latitudes .

499 The genetic distinctiveness of SE Rockall bank *L. pertusa* (observed in microsatellites and
500 ITS loci) indicates a more complicated history. The rarity of the dominant haplotype in SE
501 Rockall bank suggests either another source for colonisation or strong post-colonisation drift.
502 Approximate Bayesian computation favours an evolutionary scenario whereby the SE Rockall
503 population is colonised via admixture of the Bay of Biscay group and West Mediterranean
504 corals at approximately the time of the onset of the modern Atlantic Meridional Overturning
505 Circulation (AMOC; Repschläger et al., 2017). Mediterranean Water travelling northwards
506 along the Iberian Peninsula and Bay of Biscay does not reach the SE Rockall bank (Frank et
507 al., 2009). Instead, SE Rockall hydrodynamics are more influenced by northward moving
508 Atlantic waters, including the rich North Atlantic Current (NAC). The NAC is part of the Gulf
509 Stream, which may provide occasional genetic material from the West North Atlantic
510 *L. pertusa* reefs (Morrison et al., 2011). Analyses encompassing the full distributional range
511 of *L. pertusa* are essential to clarify missing links in population relatedness at trans-Atlantic
512 scales.

513 The ancient divergence of Mediterranean *L. pertusa* populations from the eastern and
514 western basins estimated by the ABC model to have taken place during the Last Glacial
515 Maximum (approximately 24 ka) is reasonable. In the temperate Eastern Atlantic, including
516 the Mediterranean Sea, CWC growth persisted over glacial-interglacial cycles (Frank et al.,
517 2011). This steady allopatry may have been maintained by vicariance driven by ocean
518 currents acting upon the earliest life stage of *L. pertusa* or by local adaptations. Finer-scale
519 analyses are needed to identify and quantify the importance of such variables. All together,
520 the data support a post-glacial recolonisation of the NE Atlantic by *L. pertusa*. Mediterranean
521 *L. pertusa* are divergent from most NE Atlantic populations (ITS, microsatellites). Given that
522 sampling is at best partial, it is difficult to speculate about the precise origin of the NE Atlantic
523 populations. The Mediterranean lineages and genotypes found in low proportions across the
524 NE Atlantic reefs and the high haplotypic diversity mainly in the western basin of the
525 Mediterranean Sea, concur with ABC analyses that the glacial refugia for NE Atlantic
526 *L. pertusa* colonisation may have been in the West Mediterranean Sea or in adjacent regions
527 (e.g., the coral mounds in the Gulf of Cadiz and NW Africa; Eisele *et al.*, 2011).
528 *Lophelia pertusa* populations in this region thrived during glacial periods and might have
529 provided larvae that dispersed in Mediterranean Water northwards towards the Bay of Biscay
530 (Fig. 1).

531 In contrast, *M. oculata* populations are more strongly structured and there is no evidence of a
532 large demographic expansion.

533 ## Scenario ii)

534 Concurrent to *L. pertusa*, Mediterranean Sea *M. oculata* populations were the main source
535 from which all other NE Atlantic populations emerged around the end of the LGM, as
536 estimated by model-based inference (Fig. 1 top inset). Mediterranean *M. oculata*, having
537 persisted during glacial periods (Gulf of Cadiz, NW Africa), thus represent a putative LGM
538 refugium, possibly in combination with unsampled adjacent populations. For *L. pertusa*, the
539 absence of samples from the NW coast of Africa prevented the role of this potential refugium
540 from being inferred. The estimated time for NE Atlantic colonisation, approximately 21 ka,
541 suggests that Mediterranean *M. oculata* represent a "stable rear-edge" population (Hampe &

542 Petit 2005). The Mediterranean harbours high levels of DNA diversity and the greatest
543 number of unique haplotypes and private alleles, a testament to the long-term stability of
544 Mediterranean populations (Hewitt 2000). However, unlike *L. pertusa*, there is no substantial
545 differentiation of East and West Mediterranean *M. oculata*, a difference possibly linked to
546 differences in the population size or reproductive or early life traits of these species.
547 Information on reproduction and early life history is needed to reduce model uncertainty and
548 allow a better understanding of CWC past and present connectivity.

549 Analyses gave the most support to the hypothesis that *M. oculata*'s northern range edge was
550 colonised in a stepping-stone manner (Bay of Biscay, followed by SE Rockall and later the
551 High latitudes) instead of via long-range colonisation directly from glacial refugia, as
552 supported in the case of the *L. pertusa* northern populations. Unique haplotypes were almost
553 evenly spread across the distribution range, suggesting that *M. oculata* maintained other
554 glacial (cryptic) refugia throughout its current range and underwent only localized, modest,
555 post-glacial expansions. This resulted in the co-existence of divergent genetic lineages
556 across the NE Atlantic, i.e., one lineage dominating the higher latitudes and another lineage
557 in the Bay of Biscay, both with a lower frequency in other regions. This pattern is consistent
558 with the persistence of *M. oculata* in several distinct areas, locally or regionally, followed by
559 the redistribution of divergent lineages after periods of allopatry (Petit et al., 2003). The low
560 occurrence of unique haplotypes and alleles is the result of relatively recent admixture and
561 colonisation events (Mid-Atlantic, High latitudes), which ABC analysis indicates took place
562 during the late Holocene. The large-scale spatial genetic structure would then have been
563 shaped by refugium-driven vicariance. Long-distance dispersal and gene flow, which would
564 erase patterns of population structure may be unlikely in *M. oculata*. This may be the case if
565 this species of CWC presents different reproduction and dispersal modes compared to
566 *L. pertusa*, e.g., a shorter pelagic larval duration or brooding in *M oculata* than in *L. pertusa*.
567 This hypothesised poor dispersal ability of *M. oculata* may be associated with the complex
568 habitat geomorphology (canyons, seamounts) along the NE Atlantic, along with the large
569 depth gradient (hundreds to thousands of metres) and may contribute to fragmentation,
570 reduce gene flow and maintain or reinforce large-scale patterns of the NE Atlantic population
571 structure in *M. oculata*. For instance, Lampaul canyon has the highest composition of soft
572 substrate and a near absence of coral framework compared to the other Bay of Biscay
573 canyons studied here (van den Beld et al., 2017). Such differences may have created (past)
574 barriers to gene flow. However, separating the exact effects of geography and the
575 environment on population structure is difficult, and this study identified no clear relationship
576 between divergence and depth. Finer-scale analyses are needed to identify and quantify the
577 contributions of environmental variables and putative allopatric refugia.

578 The formation of the admixed Mid-Atlantic population of *M. oculata* (Fig. 2) was dated to c. 2
579 ka (0.7–11 ka); even accounting for the wide confidence interval of the estimated time, this
580 period is well within the Holocene. During this period, the modern AMOC was established
581 and might have contributed to the colonisation of deep coral habitats along the Mid-Atlantic
582 Ridge and/or to admixture with older populations from either the European margins (SE
583 Rockall bank, Bay of Biscay canyons) or the NW Atlantic (not sampled here). The southward
584 branch of the vigorous NAC may have favoured the link between the European margins and
585 the Mid-Atlantic. The absence of Mediterranean ancestry and the level of High latitudes
586 ancestry in the Mid-Atlantic and SE Rockall regions suggest limited connection with
587 Mediterranean populations. The fact that genetic polymorphism is consistently shared
588 between European margins and the Mid-Atlantic makes it tempting to speculate on the
589 colonisation or introgression of the Mid-Atlantic by some NE Atlantic populations. However,
590 such a model may be overly simplistic, as our sampling is very fragmentary and admixture
591 patterns are complex, with potentially multiple sources located on both sides of the North
592 Atlantic. The lower coral abundance and available habitat in the Mid-Atlantic site compared to

593   the NE Atlantic margins may have further contributed to post-colonisation drift. More detailed
594   analyses of the Atlantic CWC, including analyses of samples from more locations, are
595   needed to clarify the North Atlantic phylogeography of the deep-sea.

596   The timing difference in the High latitude colonisation of *L. pertusa* and *M. oculata* may be
597   linked to differences in environmental tolerance. According to ABC analysis, *L. pertusa*
598   reached high latitudes at the end of the LGM (*c.* 21 ka; 9-29 ka), whereas the genetic
599   footprints of a possible colonisation of higher latitudes by the SE Rockall populations of *M.*
600   *oculata* suggest a much more recent event (*c.* 0.3 ka, 0.07-3 ka). In fact, *L. pertusa* has
601   thermal acclimation via respiration and calcification mechanisms that are absent in
602   *M. oculata* (Nauman et al., 2014), and *L. pertusa*'s relative abundance increases from the
603   Mediterranean to Icelandic waters (Arnaud-Haond et al., 2017). The Holocene colonisation of
604   the high latitudes of Europe (e.g., Norway; Fig. 1) is well documented (Schröder-Ritzrau et
605   al., 2005).

606   In any case, ABC model-based inferences rely on assumptions that cannot easily be
607   controlled in natural populations. Our findings should be interpreted as probable hypotheses
608   rather than clear evidence of past demographic events and detailed roads of colonization.
609   Further theoretical and experimental work that can contribute to a better understanding of
610   CWC phylogeography and connectivity (e.g., early life history traits) is needed. Analyses
611   making use of more widespread samples at the Atlantic scale and high-density data will allow
612   the reconstruction of the phylogeographic history of CWC with more precision. Moreover, our
613   study highlights the need to explore the genetic nature of CWC in the western Mediterranean
614   (Alboran Sea) and the Gulf of Cadiz to determine their possible contributions to larval
615   connectivity and past re-colonisation of the NE Atlantic.

616   **Conclusion** The genetic data presented here from deep-sea corals from European margins
617   provide new insights into CWC population history. Our results support a northward post-Last
618   Glacial Maximum expansion of *Lophelia pertusa* and *Madrepora oculata* from the West
619   Mediterranean Sea into the NE Atlantic margin. While the moderate to high gene flow of
620   *L. pertusa* homogenized nearly the whole Atlantic genetic pool, *M. oculata* seems to have
621   progressed slower than *L. pertusa*, particularly in High latitudes and might have been
622   additionally recolonised from other areas. According to the present estimations, *L. pertusa*
623   expanded swiftly along the NE Atlantic at a rate of 0.7 to 2 km per year (considering
624   4,000 km of expansion in the past 10 to 30 ka). The period of Atlantic-Mediterranean
625   separation led to strong genetic differentiation between extant coral populations in the
626   respective regions. This differentiation can be explained by either a founder effect at the NE
627   Atlantic or an unsampled genetic source in the Mediterranean Sea or around NW Africa. The
628   remarkable mosaic of distinct genotypes of *M. oculata* supports the existence of a more
629   complex history, shaped by putative cryptic refugia, admixture, possible different dispersal
630   abilities and reproductive (in)compatibilities. Because of current data limitations, it is not yet
631   possible to determine the most important factor underlying the apparent lack of gene flow
632   along the European margin for *M. oculata* populations. Further CWC samples from the North
633   Atlantic are needed in order to better understand the extent to which these signals of
634   migration and admixture are representative of North Atlantic CWC as a whole. Nonetheless,
635   the contrasting patterns of genetic diversity observed here strongly support differing present-
636   day dispersals of *L. pertusa* and *M. oculata* and that past environmental changes had
637   different influences on these CWC species. Our study provides an important warning for
638   managers that even taxa with seemingly similar ecological roles, geographic distributions and
639   tolerances may differ in their response to global change. Therefore, multi-species models are
640   required to ensure conservation measures, such as truly representative and connected
641   networks of marine protected Areas.

642 Author contributions: RB, SAH and JRHB conceived the ideas; RB, SAH, JRHB, NF, MT, AS,
643 AG and ALM, carried out fieldwork; RB, SAH, JRHB, JFB collected the data; RB, SAH,
644 JRHB, MC, JFB and NF analysed the data; JRHB, RB and SAH led the writing. All authors
645 read and approved the final manuscript.

Data Accessibility Statement

647 Microsatellite and sequence data are accessible online at GenBank under accession
648 numbers SUB5134195 and SUB5108670; and on DRYAD .

649 **viii. Tables and captions**

650 Table 1 - Genetic diversity at microsatellite loci for North-East Atlantic *Lophelia pertusa*. n - sample size; Âr - allelic richness; Âr(5) -
651 standardized allelic richness to the lowest sample size (N=5); Âp - private allelic richness; He and Ho - expected and observed heterozygosity
652 respectively; Fis - departure from HWE. P-values below 0.05, 0.01 and 0.001 are represented by *, ** and ***, respectively.

Region	Site	n	Âr	Âr(5)	Âp	He	Ho	Fis
Eastern Mediterranean Sea	Santa Maria di Leuca (SML)	12	8.1	6.0 ± 0.2	4	0.80 ± 0.06	0.71 ± 0.31	0.15***
Western Mediterranean Sea	Lacaze-Duthiers canyon (LCD)	7	4.9	4.9 ± 0.00	2	0.72 ± 0.13	0.84 ± 0.19	-0.10
Bay of Biscay	Croisic canyon (CRS)	30	18.9	8.8 ± 0.12	5	0.89 ± 0.07	0.80 ± 0.14	0.12***
Bay of Biscay	Guilvinec canyon (GUI)	34	18.3	8.7 ± 0.12	4	0.89 ± 0.08	0.86 ± 0.04	0.05**
Bay of Biscay	Lampaul canyon (LMP)	7	8.8	8.8 ± 0.00	2	0.83 ± 0.09	0.80 ± 0.19	0.11**
Bay of Biscay	Crozon canyon (CRZ)	12	11.0	8.0 ± 0.13	2	0.84 ± 0.09	0.74 ± 0.14	0.16***
Bay of Biscay	Morgat-Douarnez canyon (MRG)	20	16.4	8.6 ± 0.16	4	0.87 ± 0.09	0.83 ± 0.20	0.07**
Bay of Biscay	Petite Sole 1 canyon (PS1)	26	17.4	8.7 ± 0.12	5	0.88 ± 0.09	0.83 ± 0.11	0.07***
Bay of Biscay	Petite Sole 2 canyon (PS2)	27	17.5	8.9 ± 0.10	4	0.90 ± 0.06	0.85 ± 0.09	0.07***
SE Rockall bank	Logachev Mounds (LOG)	22	14.8	8.1 ± 0.12	2	0.87 ± 0.07	0.77 ± 0.13	0.14***
High latitudes	Londsjup 1 (LON1)	7	8.5	8.5 ± 0.00	1	0.82 ± 0.09	0.77 ± 0.15	0.14**
High latitudes	Londsjup 2 (LON2)	20	14.5	8.2 ± 0.12	4	0.86 ± 0.10	0.74 ± 0.16	0.17***
High latitudes	Hafadsjup (HAF)	16	13.6	8.5 ± 0.12	1	0.89 ± 0.05	0.70 ± 0.22	0.25***

653

654 Table 2 - Genetic diversity at microsatellite loci for North-East Atlantic *Madrepora oculata*. n - sample size; Âr - allelic richness; Âr(5) -
655 standardized allelic richness to the lowest sample size (N=5); Âp - private allelic richness; He and Ho - expected and observed heterozygosity
656 respectively; Fis - departure from HWE. P-values below 0.05, 0.01 and 0.001 are represented by *, ** and ***, respectively.

Region	Site	n	Âr	Âr(5)	Âp	He	Ho	Fis
Eastern Mediterranean Sea	Montenegro (MNG)	5	2.3	2.3 ± 0.0	2	0.31 ± 0.34	0.27 ± 0.39	0.26
Western Mediterranean Sea	Lacaze-Duthiers canyon (LCD)	6	3.5	3.3 ± 0.04	4	0.45 ± 0.32	0.56 ± 0.40	-0.16
Mid Atlantic Ocean	Azores (AZO)	5	2.7	2.7 ± 0.0	0	0.38 ± 0.27	0.47 ± 0.39	-0.12
Bay of Biscay	Croisic canyon (CRS)	39	6.3	3.7 ± 0.06	1	0.66 ± 0.10	0.67 ± 0.13	0.00
Bay of Biscay	Guilvinec canyon (GUI)	42	5.5	3.7 ± 0.06	0	0.67 ± 0.15	0.60 ± 0.28	0.12***
Bay of Biscay	Lampaul canyon (LMP)	11	3.8	3.2 ± 0.03	1	0.56 ± 0.28	0.58 ± 0.31	0.02
Bay of Biscay	Morgat-Douarnez canyon (MRG)	29	4.8	3.5 ± 0.05	0	0.61 ± 0.16	0.56 ± 0.23	0.10*
Bay of Biscay	Crozon canyon (CRZ)	23	5.5	3.5 ± 0.06	1	0.59 ± 0.24	0.52 ± 0.27	0.14**

Bay of Biscay	Petite Sole 1 canyon (PS1)	23	5.2	3.6 ± 0.05	0	0.63 ± 0.16	0.65 ± 0.21	-0.01
Bay of Biscay	Petite Sole 2 canyon (PS2)	32	6.2	3.7 ± 0.08	0	0.65 ± 0.14	0.59 ± 0.19	0.10*
SE Rockall bank	Logachev Mounds (LOG)	24	6.0	3.5 ± 0.07	0	0.54 ± 0.30	0.49 ± 0.31	0.11*
High latitudes	Londsjup 1 (LON1)	6	3.7	3.3 ± 0.04	0	0.45 ± 0.30	0.39 ± 0.29	0.22*
High latitudes	Londsjup 2 (LON2)	33	4.5	2.5 ± 0.06	2	0.38 ± 0.28	0.31 ± 0.30	0.18**
High latitudes	Hafadsjup (HAF)	17	4.5	3.1 ± 0.06	0	0.46 ± 0.32	0.44 ± 0.34	0.06

657

658 Table 3 - Genetic diversity and neutrality tests for the internal transcribed spacer ribosomal sequences at each North-East Atlantic location of
659 *Lophelia pertusa*. Asterisk (*) - P-values under 0.05. NA - not applicable (Lampaul canyon had no polymorphic sites).

660

	No. Samples (n)	No. Haplotypes	No. Private haplotypes	Haplotype diversity (H)	Nucleotide diversity (π)	Tajima's D	FS
East Mediterranean Sea							
Santa Maria di Leuca (SML)	15	4	0	0.4476	0.0011	-0.33	1.52
West Mediterranean Sea							
Lacaze-Duthiers canyon (LCD)	7	6	2	0.7143	0.0028	-0.86	0.75
Bay of Biscay							
Croisic canyon (CRS)	21	6	2	0.2714	0.0003	-1.73*	-2.82*
Guilvinec canyon (GUI)	23	7	1	0.249	0.0004	-1.88*	-1.75*
Morgat-Douarnez canyon (MRG)	30	10	4	0.2529	0.0003	-2.01*	-3.70*
Crozon canyon (CRZ)	11	6	2	0.6182	0.0014	-1.85*	-0.92
Lampaul canyon (LMP)	7	1	0	0	NA	NA	NA
Petite Sole1 (PS1)	28	3	1	0.0909	0.0001	-1.16	-0.96
Petite Sole2 (PS2)	22	5	2	0.2063	0.0004	-1.89*	-1.62*
SE Rockall bank							
Logachev mounds (LOG)	21	5	3	0.4143	0.0006	-1.22	-1.01
High							

latitudes

|							
Londsjup1 (LON1)	8	4	2	0.4643	0.0007	-1.45	-0.30
Londsjup2 (LON2)	20	7	2	0.5105	0.0008	-1.41	-1.48
HafadJup (HAF)	16	5	1	0.4417	0.0008	-1.22	-0.37
Mean	14.5	5.5	1.7	0.4	0.0008	-0.78	-1.50
s.d.	8.95	1.90	1.11	0.20	0.00073	0.991	1.594

661

662 Table 4 - Genetic diversity and neutrality tests for the internal transcribed spacer ribosomal sequences at each North-East Atlantic location of
663 *Madrepora oculata*. Asterisk (*) - P-values under 0.05. NA - not applicable (Londsjup 2 had no polymorphic sites).

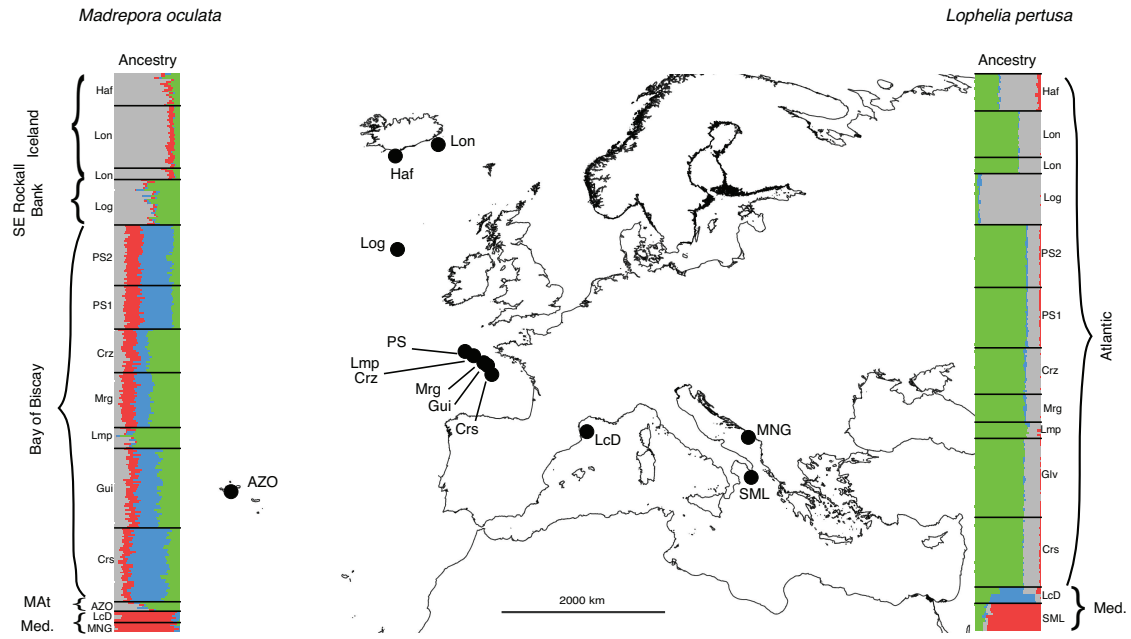|	No. Samples (n)	No. Haplotypes	No. Private haplotypes	Haplotype diversity (H)	Nucleotide diversity (π)	Tajima's D	FS
East Mediterranean Sea	5	5	4				
Montenegro (MNG)	5	5	4	0.71	0.0018	-1.55*	-0.13
West Mediterranean Sea	4	4	4				
Lacaze-Duthiers canyon (LCD)	4	4	4	0.83	0.0025	0.37	0.65
Mid Atlantic Ocean	5	4	2				
Azores (AZO)	5	4	2	0.90	0.0020	-0.56	-0.85
Bay of Biscay	91	33	8				
Croisic canyon (CRS)	10	10	0	0.60	0.0011	0.47	0.84
Guilvinec canyon (GUI)	20	16	2	0.68	0.0016	0.25	-0.43
Morgat-Douarnez canyon (MRG)	10	13	0	0.56	0.0013	0.30	0.17
Crozon canyon (CRZ)	12	8	0	0.14	0.0004	-1.67*	0.90
Lampaul canyon (LMP)	10	10	2	0.47	0.0010	-0.64	0.83
Petite Sole1 (PS1)	7	8	2	0.64	0.0014	0.23	1.23
Petite Sole2 (PS2)	12	12	2	0.42	0.0010	-1.73	-0.16
SE Rockall bank	27	21	2				
Logachev mounds (LOG)	27	21	2	0.66	0.0014	-0.46	-0.51
High latitudes	63	12	4				
Londsjup1 (LON1)	8	8	2	0.68	0.0018	-0.49	1.65
Londsjup2 (LON2)	34	4	0	NA	NA	N.A.	N.A.
HafadJup (HAF)	21	8	2	0.27	0.0006	-1.02	0.53
Mean	14.1	11.4	2.4	0.58	0.0014	-0.46	0.34
s.d.	8.90	6.82	1.90	0.212	0.00057	0.784	0.722

ix. Figures and captions

665 Figure 1 - Contemporary distribution of *M. oculata* (black diamonds) and *L. pertusa* (grey
666 circles) in the NE Atlantic (2017 UNEP database; http://data.unep-wcmc.org) and the paths
667 of the main North East Atlantic Ocean currents (adapted from Montero-Serrano et al., 2011,
668 Somoza et al., 2014 and Cossa et al., 2018): MOW - Mediterranean Outflow Water; MW -
669 Mediterranean Sea Water; NAC - North Atlantic Water; MNAW - Modified North Atlantic
670 Water; EAAIW - Eastern Antarctic Intermediate Water; LSW - Labrador Sea Water; ISOW -
671 Iceland-Scotland Overflow Water. Site abbreviations are as in Table 1. Dates correspond to
672 estimated ages for coral mound growth (adapted from Schröder-Ritzrau et al., 2005). Insets
673 are the selected demographic history models for each cold-water coral species. ka -
674 thousand years ago. Map was created on QGIS with Mollweide's equal area projection.
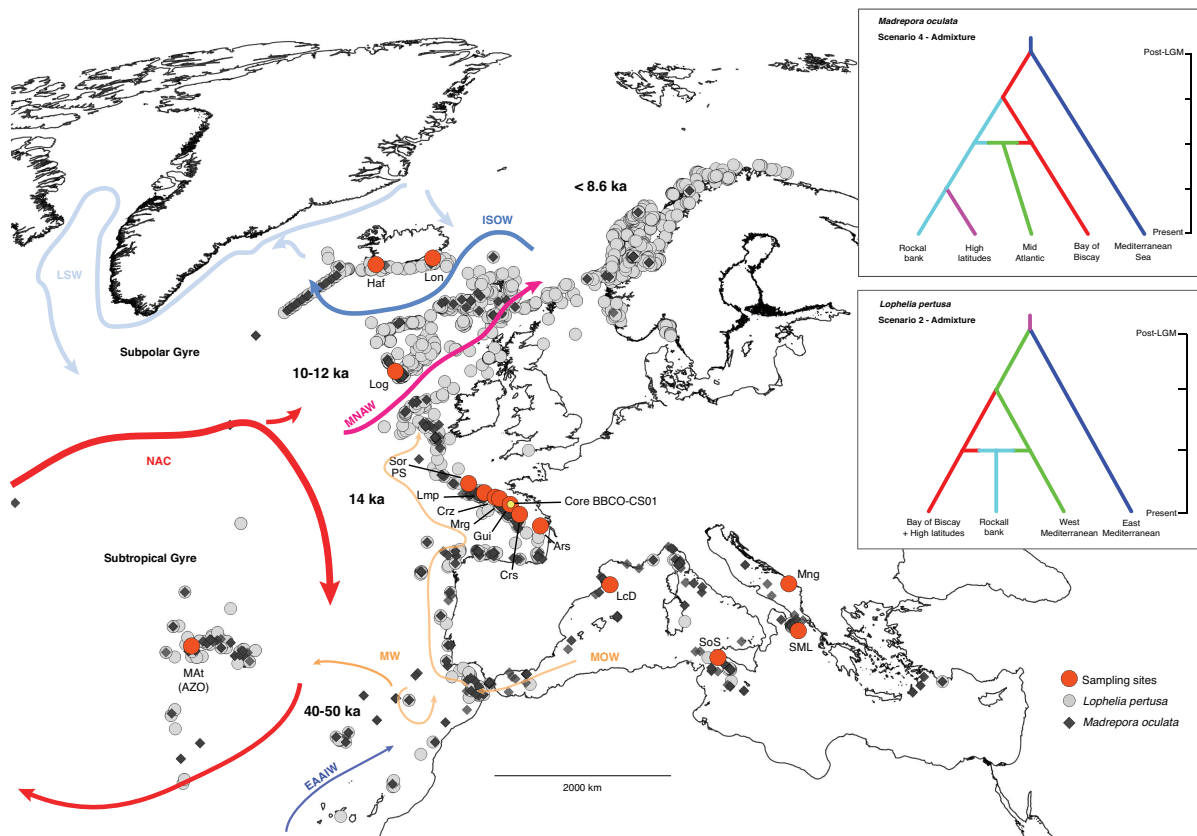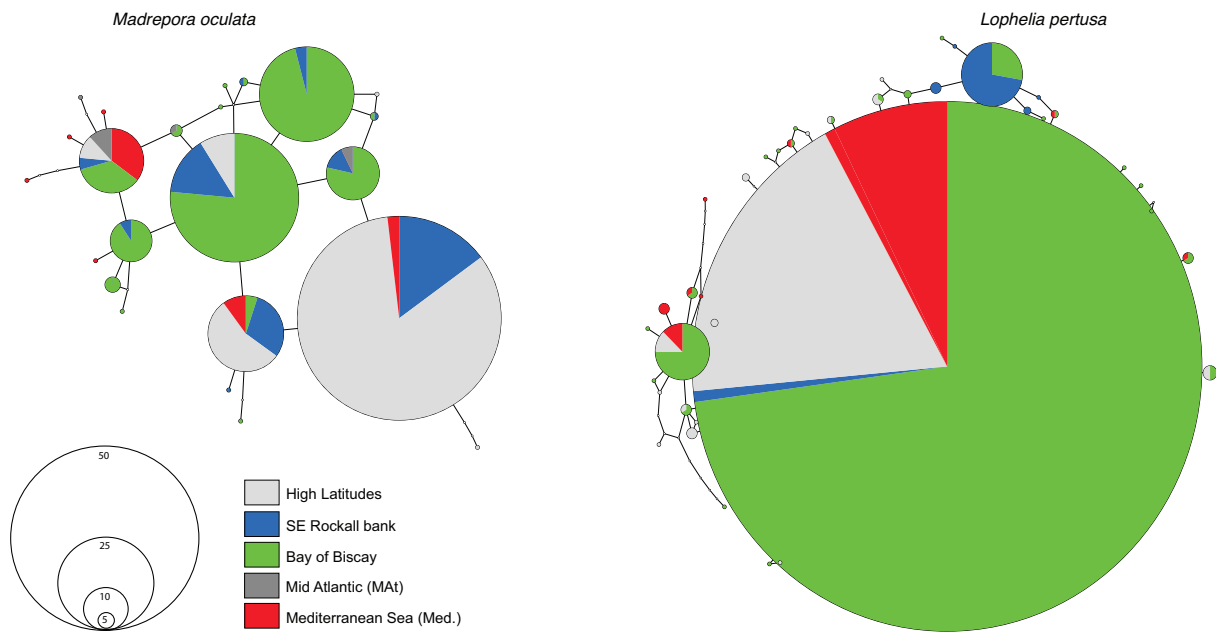

675
676
677
678
679
680
681
682
683
684

685   Figure 2 - Genetic subdivisions among regional samples. (a) Microsatellite population
686   ancestry diagrams from TESS displaying the probability of each individual in K = 4 clusters
687   for *Madrepora oculata* (left) and *Lophelia pertusa* (right) (clusters denoted by different
688   colours). Each individual is depicted by a horizontal line partitioned into K coloured sections,
689   and the length of each section is proportional to the estimated ancestry probability for each
690   cluster. Sample names refer to the sites indicated in Table 1 and Fig. 1. Samples from the
691   Bay of Biscay canyons (left diagram) are geographically ordered from north to south
692   according to Fig. 1. Black horizontal lines separate adjacent sites (MAt - Mid-Atlantic, Med. -
693   Mediterranean). (b) Parsimony haplotype networks of internal transcribed spacer ribosomal
694   sequences for *M. oculata* (left) and *L. pertusa* (right). The size of the circle is proportional to
695   the observed number of sequences for the corresponding haplotype. Pie charts illustrate the
696   proportion of a haplotype found in each region. The length of links is proportional to the
697   number of mutations separating two haplotypes; the shortest length represents a single
698   mutation. Mediterranean data include eastern and western basin samples.

a

Madrepora oculata

Ancestry

Lophelia pertusa

Ancestry

Iceland — Haf, Lon, Lon, Log
SE Rockall Bank
PS2, PS1, Crz, Mrg, Lmp, Gui, Crs — Bay of Biscay
AZO
MAt — AZO
Med. — LcD, MNG

Haf, Lon, Lon, Log, PS2, PS1, Crz, Mrg, Lmp, Glv, Crs — Atlantic
LcD, SML — Med.

Lon
Haf
Log
PS
Lmp
Crz
Mrg
Gui
Crs
AZO
LcD
MNG
SML

2000 km

b

Madrepora oculata

Lophelia pertusa

50
25
10
5

High Latitudes
SE Rockall bank
Bay of Biscay
Mid Atlantic (MAt)
Mediterranean Sea (Med.)

699
700
701
702
703
704
705
706
707
708

21

Figure 3 - Genetic subdivisions among NE Atlantic cold-water coral samples. Top - discriminant analyses of principal components (DAPC) for *Madrepora oculata* and *Lophelia pertusa*. A minimum-spanning tree based on the squared distances between groups connects group centres (crosses). Insets show the variance explained by the principal components included in the analyses (black). Because the identified optimal number of genetic clusters (K) for *L. pertusa* is K=2 (see additional inset with sample density along the first discriminant function), the DAPC plot for *L. pertusa* shows samples colour-coded by sampling site. Bottom - population membership diagrams displaying the probability of each individual colour-coded by sampling site.

a) *Madrepora oculata*

b) *Lophelia pertusa*
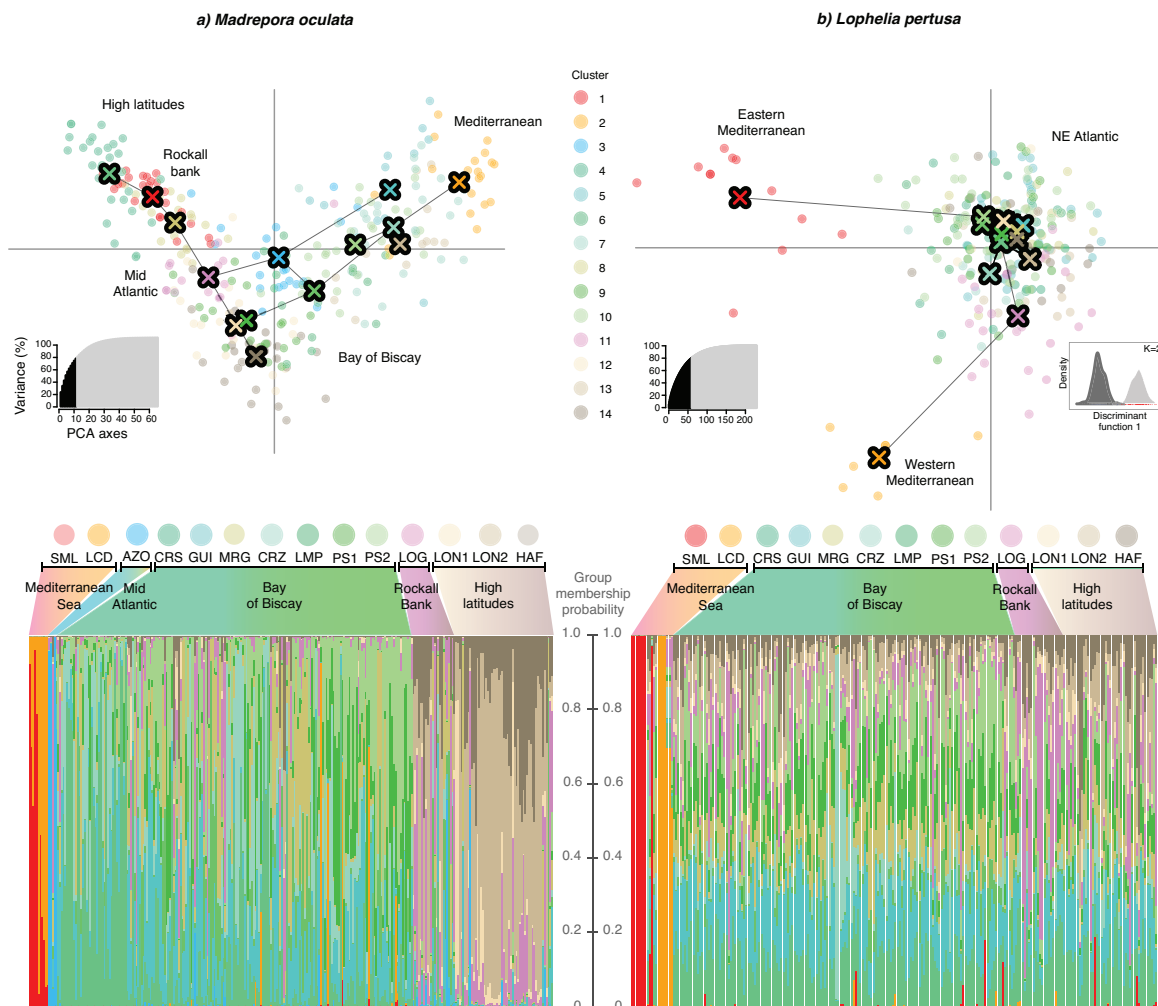
729 **x. References**

730 Arnaud-Haond, S., Van den Beld, I.M.J., Becheler, R., Orejas, C., Menot, L., Frank, N., Grehan, A. &
731   Bourillet, J.F. (2017) Two "pillars" of cold-water coral reefs along Atlantic European margins:
732   Prevalent association of Madrepora oculata with Lophelia pertusa, from reef to colony scale.
733   *Deep-Sea Research Part II: Topical Studies in Oceanography*, **145**, 110–119.

734 Becheler, R., Cassone, A.L., Noël, P., Mouchel, O., Morrison, C.L. & Arnaud-Haond, S. (2017) Low
735   incidence of clonality in cold water corals revealed through the novel use of a standardized
736   protocol adapted to deep sea sampling. *Deep-Sea Research Part II: Topical Studies in*
737   *Oceanography*, **145**, 120–130.

738 van den Beld, I.M.J., Bourillet, J.-F., Arnaud-Haond, S., de Chambure, L., Davies, J.S., Guillaumont,
739   B., Olu, K., & Menot, L. (2017) Cold-Water Coral Habitats in Submarine Canyons of the Bay of
740   Biscay. *Frontiers in Marine Science*, **4**.

741 Belkhir K., Borsa P., Chikhi L., Raufaste N., B.F. (2004) Genetix 4.05, logiciel sous Windows TM pour
742   la génétique des populations.

743 Bouchet, P. & Taviani, M. (1992) The Mediterranean deep-sea fauna: pseudopopulations of Atlantic
744   species? *Deep Sea Research Part A, Oceanographic Research Papers*, **39**, 169–184.

745 Caye, K., Jay, F., Michel, O., & François, O. (2016) Fast inference of individual admixture coefficients
746   using geographic data. *bioRxiv preprint*, 1–35.

747 Chen, C., Durand, E., Forbes, F. & François, O. (2007) Bayesian clustering algorithms ascertaining
748   spatial population structure: a new computer program and a comparison study. *Molecular*
749   *Ecology Notes*, **7**, 747–756.

750 Clement, M., Posada, D., & Crandall, K.A. (2000) TCS: A computer program to estimate gene
751   genealogies. *Molecular Ecology*, **9**, 1657–1659.

752 Clark, P.U. (2009) The Last Glacial Maximum. *Science*, **325**, 710–714.

753 Cordes, E.E., Jones, D.O., Schlacher, T.., Amon, D.J., Bernardino, A.F., Brooke, S., Carney, R.,
754   DeLeo, D.M., Dunlop, K.M., Escobar-Briones, E.G., Gates, A.R., Genio, L., Gobin, J., Henry, L.-
755   A., Herrera, S., Hoyt, S., Joye, S., KArk, S., Mestre, N.C., Metaxas, A., Pfeifer, S., Sink, K.,
756   Sweetman, A.K. & Witte, U.F. (2016) Environmental impacts of the deep-water oil and gas
757   industry: a review to guide management strategies. *Frontiers in Environmental Science*, **4**, 1–54.

758 Cornuet, J.M., Pudlo, P., Veyssier, J., Dehne-Garcia, A., Gautier, M., Leblois, R., Marin, J.M., &
759   Estoup, A. (2014) DIYABC v2.0: A software to make approximate Bayesian computation
760   inferences about population history using single nucleotide polymorphism, DNA sequence and
761   microsatellite data. *Bioinformatics*, **30**, 1187–1189.

762 Cossa, D., Heimbürger, L.E., Pérez, F.F., García-Ibáñez, M.I., Sonke, J.E., Planquette, H., Lherminier,
763   P., Boutorh, J., Cheize, M., Lukas Menzel Barraqueta, J., Shelley, R., & Sarthou, G. (2018)
764   Mercury distribution and transport in the North Atlantic Ocean along the GEOTRACES-GA01
765   transect. *Biogeosciences*, **15**, 2309–2323.

766 Dahl, M.P., Pereyra, R.T., Lundälv, T. & André, C. (2012) Fine-scale spatial genetic structure and
767   clonal distribution of the cold-water coral Lophelia pertusa. *Coral Reefs*, **31**, 1135–1148.

768 Diekmann, O.E., Bak, R.P.M., Stam, W.T. & Olsen, J.L. (2001) Molecular genetic evidence for
769   probable reticulate speciation in the coral genus Madracis from a Caribbean fringing reef slope.
770   *Marine Biology*, **139**, 221–233.

771 Doyle, J.J. & Doyle, J.L. (1988) Natural interspecific hybridization in eastern north-american Claytonia.
772   *American Journal of Botany*, **75**, 1238–1246.

773 Drummond, A.J., Rambaut, A., Shapiro, B., & Pybus, O.G. (2005) Bayesian coalescent inference of
774   past population dynamics from molecular sequences. Molecular Biology and Evolution, 22,
775   1185–1192.

776 Dullo, W.C., Flögel, S. & Rüggeberg, A. (2008) Cold-water coral growth in relation to the hydrography
777   of the Celtic and Nordic European continental margin. *Marine Ecology Progress Series*, **371**,
778   165–176.

779 Eisele, M., Frank, N., Wienberg, C., Hebbeln, D., López Correa, M., Douville, E. & Freiwald, A. (2011)
780   Productivity controlled cold-water coral growth periods during the last glacial off Mauritania.
781   *Marine Geology*, **280**, 143–149.

782 Excoffier, L., Laval, G. & Schneider, S. (2005) Arlequin (version 3.0): An integrated software package
783   for population genetics data analysis. *Evolutionary Bioinformatics Online*, **1**, 47–50.

784 Fenberg, P.B., Caselle, J.E., Claudet, J., Clemence, M., Gaines, S.D., Antonio García-Charton, J.,
785   Gonçalves, E.J., Grorud-Colvert, K., Guidetti, P., Jenkins, S.R., Jones, P.J.S., Lester, S.E.,
786   McAllen, R., Moland, E., Planes, S. & Sorensen, T.K. (2012) The science of European marine
787   reserves: Status, efficacy, and future needs. *Marine Policy*, **36**, 1012–1021.

788 Fink, H.G., Wienberg, C., De Pol-Holz, R., Wintersteller, P. & Hebbeln, D. (2013) Cold-water coral
789   growth in the Alboran Sea related to high productivity during the Late Pleistocene and Holocene.
790   *Marine Geology*, **339**, 71–82.

791 Flot, J.-F., Dahl, M. & André, C. (2013) Lophelia pertusa corals from the Ionian and Barents seas
792   share identical nuclear ITS2 and near-identical mitochondrial genome sequences. *BMC research
793   notes*, **6**, 144.

794 François, O., Ancelet, S. & Guillot, G. (2006) Bayesian clustering using hidden Markov random fields
795   in spatial population genetics. *Genetics*, **174**, 805–16.

796 Frank, N., Ricard, E., Lutringer-Paquet, A., van der Land, C., Colin, C., Blamart, D., Foubert, A., Van
797   Rooij, D., Henriet, J.P., de Haas, H. & van Weering, T. (2009) The Holocene occurrence of cold
798   water corals in the NE Atlantic: Implications for coral carbonate mound evolution. *Marine
799   Geology*, **266**, 129–142.

800 Frank, N., Freiwald, A., Correa, M.L., Wienberg, C., Eisele, M., Hebbeln, D., Van Rooij, D., Henriet, J.-
801   P., Colin, C., van Weering, T., de Haas, H., Buhl-Mortensen, P., Roberts, J.M., De Mol, B.,
802   Douville, E., Blamart, D., & Hatte, C. (2011) Northeastern Atlantic cold-water coral reefs and
803   climate. *Geology*, 39, 743–746.

804 Fu, Y.X. (1996) New statistical tests of neutrality for DNA samples from a population. *Genetics*, **143**,
805   557–570.

806 Henry, L.A., Frank, N., Hebbeln, D., Wienberg, C., Robinson, L., de Flierdt, T. van, Dahl, M., Douarin,
807   M., Morrison, C.L., Correa, M.L., Rogers, A.D., Ruckelshausen, M. & Roberts, J.M. (2014) Global
808   ocean conveyor lowers extinction risk in the deep sea. *Deep-Sea Research Part I:
809   Oceanographic Research Papers*, **88**, 8–16.

810 Herrera, S., Shank, T.M. & Sanchez, J.A. (2012) Spatial and temporal patterns of genetic variation in
811   the widespread antitropical deep-sea coral Paragorgia arborea. *Molecular Ecology*, **21**, 6053–
812   6067.

813 Hewitt, G.M. (2004) Genetic consequences of climatic oscillations in the Quaternary. *Philosophical
814   Transactions of the Royal Society B: Biological Sciences*, **359**, 183–195.

815 Hewitt, G.M. (1999) Post-glacial re-colonisation of European biota. *Biological Journal of the Linnean
816   Society*, **68**, 87–112.

817 Hewitt, G.M. (1996) Some genetic consequences of ice ages, and their role, in divergence and
818   speciation. *Biological Journal of the Linnean Society*, **58**, 247–276.

819 Jombart, T. (2008) Adegenet: A R package for the multivariate analysis of genetic markers.
820   *Bioinformatics*, **24**, 1403–1405.

821 Jombart, T., Devillard, S., & Balloux, F. (2010) Discriminant analysis of principal components: a new
822   method for the analysis of genetically structured populations. *BMC genetics*, **11**, 94.

823 Kearse, M., Moir, R., Wilson, A., Stones-Havas, S., Cheung, M., Sturrock, S., Buxton, S., Cooper, A.,
824   Markowitz, S., Duran, C., Thierer, T., Ashton, B., Meintjes, P. & Drummond, A. (2012) Geneious
825   Basic: An integrated and extendable desktop software platform for the organization and analysis
826   of sequence data. *Bioinformatics*, **28**, 1647–1649.

827 Kitahara, M. V., Cairns, S.D., Stolarski, J., Blair, D., & Miller, D.J. (2010) A comprehensive
828   phylogenetic analysis of the scleractinia (Cnidaria, Anthozoa) based on mitochondrial CO1
829   sequence data. *PLoS ONE*, 5, e11490.

830 Kousteni, V., Kasapidis, P., Kotoulas, G. & Megalofonou, P. (2015) Strong population genetic structure
831 and contrasting demographic histories for the small-spotted catshark (*Scyliorhinus canicula*) in
832 the Mediterranean Sea. *Heredity*, **114**, 333–343.

833 Larsson, A.I., Jarnegren, J., Strömberg, S.M., Dahl, M.P., Lundalv, T. & Brooke, S. (2014)
834 Embryogenesis and larval biology of the cold-water coral Lophelia pertusa. *PLoS ONE*, **9**.

835 Lartaud, F., Meistertzheim, A.L., Peru, E. & Le Bris, N. (2017) In situ growth experiments of reef-
836 building cold-water corals: the good, the bad and the ugly. *Deep Sea Research Part I:*
837 *Oceanographic Research Papers*, **121**, 70–78.

838 Lartaud, F., Pareige, S., de Rafelis, M., Feuillassier, L., Bideau, M., Peru, E., De la Vega, E.,
839 Nedoncelle, K., Romans, P. & Le Bris, N. (2014) Temporal changes in the growth of two
840 Mediterranean cold-water coral species, in situ and in aquaria. *Deep-Sea Research Part II:*
841 *Topical Studies in Oceanography*, **99**, 64–70.

842 LeGoff-Vitry, M.C., Pybus, O.G. & Rogers, A.D. (2004) Genetic structure of the deep-sea coral
843 Lophelia pertusa in the northeast Atlantic revealed by microsatellites and internal transcribed
844 space sequences. *Molecular Ecology*, **13**, 537–549.

845 Maggs, C.A., Castilho, R., Foltz, D., Henzler, C., Jolly, M.T., Kelly, J., Olsen, J., Perez, K.E., Stam, W.,
846 Väinölä, R., Viard, F. & Wares, J. (2008) Evaluating signatures of glacial refugia for north atlantic
847 benthic marine taxa. *Ecology*, **89**.

848 McCulloch, M., Taviani, M., Montagna, P., López Correa, M., Remia, A., & Mortimer, G. (2010)
849 Proliferation and demise of deep-sea corals in the Mediterranean during the Younger Dryas.
850 *Earth and Planetary Science Letters*, **298**, 143–152.

851 Meistertzheim, A.L., Lartaud, F., Arnaud-Haond, S., Kalenitchenko, D., Bessalam, M., Le Bris, N. &
852 Galand, P.E. (2016) Patterns of bacteria-host associations suggest different ecological strategies
853 between two reef building cold-water coral species. *Deep-Sea Research Part I: Oceanographic*
854 *Research Papers*, **114**, 12–22.

855 Milligan, R.J., Spence, G., Roberts, J.M. & Bailey, D.M. (2016) Fish communities associated with cold-
856 water corals vary with depth and substratum type. *Deep-Sea Research Part I: Oceanographic*
857 *Research Papers*, **114**, 43–54.

858 De Mol, B., Van Rensbergen, P., Pillen, S., Van Herreweghe, K., Van Rooij, D., McDonnell, A.,
859 Huvenne, V., Ivanov, M., Swennen, R. & Henriet, J.P. (2002) Large deep-water coral banks in
860 the Porcupine Basin, southwest of Ireland. *Marine Geology*, **188**, 193–231.

861 Montero-Serrano, J.C., Frank, N., Colin, C., Wienberg, C., & Eisele, M. (2011) The climate influence
862 on the mid-depth Northeast Atlantic gyres viewed by cold-water corals. *Geophysical Research*
863 *Letters*, **38**, L19604.

864 Morrison, C.L., Eackles, M.S., Johnson, R.L. & King, T.L. (2008) Characterization of 13 microsatellite
865 loci for the deep-sea coral, Lophelia pertusa (Linnaeus 1758), from the western North Atlantic
866 Ocean and Gulf of Mexico. *Molecular Ecology Resources*, **8**, 1037–1039.

867 Morrison, C.L., Ross, S.W., Nizinski, M.S., Brooke, S., Järnegren, J., Waller, R.G., Johnson, R.L. &
868 King, T.L. (2011) Genetic discontinuity among regional populations of Lophelia pertusa in the
869 North Atlantic Ocean. *Conservation Genetics*, **12**, 713–729.

870 Morton, B. & Britton, J.C. (2000) Origins of the Azorean Intertidal Biota: the Significance of Introduced
871 Species, Survivors of Chance Events. *Arquipélago. Life and Marine Science*, **2**, 29–51.

872 Naumann, M.S., Orejas, C., & Ferrier-Pagés, C. (2014) Species-specific physiological response by the
873 cold-water corals Lophelia pertusa and Madrepora oculata to variations within their natural
874 temperature range. *Deep-Sea Research Part II: Topical Studies in Oceanography*, **99**, 36–41.

875 Nei, M. (1978) Estimation of average heterozygosity and genetic distance from a small number of
876 individuals. *Genetics*, **89**, 583–590.

877 Nei, M. (1987) *Molecular Evolutionary Genetics*, Columbia University Press, New York, NY.

878 Petit, R.J., Aguinagalde, I., Beaulieu, J.-L. De, Bittkau, C., Brewer, S., Cheddadi, R., Ennos, R.,

Fineschi, S., Grivet, D., Lascoux, M., Mohanty, A., Muller-Starck, G., Demesure-Musch, B., Palmé, A., Martín, J.P., Rendell, S. & Vendramin, G.G. (2003) Glacial refugia: Hotspots but not melting pots of genetic diversity. *Science*, **300**, 1563–1565.

Price, J.F., Baringer, M.O., Lueck, R.G., Johnson, G.C., Ambar, I., Parrilla, G., Cantos, A., Kennelly, M.A., & Sanford, T.B. (1993) Mediterranean Outflow Mixing and Dynamics. *Science (New York, N.Y.)*, **259**, 1277–1282.

Pritchard, J.K., Stephens, M. & Donnelly, P. (2000) Inference of population structure using multilocus genotype data. *Genetics*, **155**, 945–59.

Pusceddu, A., Bianchelli, S., Martín, J., Puig, P., Palanques, A., Masqué, P. & Danovaro, R. (2014) Chronic and intensive bottom trawling impairs deep-sea biodiversity and ecosystem functioning. *Proceedings of the National Academy of Sciences of the United States of America*, **111**, 8861–6.

Quattrini, A.M., Baums, I.B., Shank, T.M., Morrison, C.L. & Cordes, E.E. (2015) Testing the depth-differentiation hypothesis in a deepwater octocoral. *Proceedings of the Royal Society B*, **282**, 20150008.

Ramos, A., Sanz, J.L., Ramil, F., Agudo, L.M. & Presas-Navarro, C. (2017) *Deep-Sea Ecosystems Off Mauritania*. *Deep-Sea Ecosystems Off Mauritania* (ed. by A. Ramos), J.L. Sanz), and F. Ramil), pp. 481–525. Springer Netherlands.

Repschläger, J., Garbe-Schönberg, D., Weinelt, M., & Schneider, R. (2017) Holocene evolution of the North Atlantic subsurface transport. *Climate of the Past*, **13**, 333–344.

Rogerson, M., Rohling, E.J., Weaver, P.P.E. & Murray, J.W. (2004) The Azores Front since the Last Glacial Maximum. *Earth and Planetary Science Letters*, **222**, 779–789.

Sabelli, B. & Taviani, M. (2014) *The making of the Mediterranean Molluscan Biodiversity*. *The Mediterranean Sea: Its History and Present Challenges* (ed. by S. Goffredo) and Z. Dubinsky), pp. 1–678.

Santos, A., Cabezas, M.P., Tavares, A.I., Xavier, R., & Branco, M. (2015) TcsBU: A tool to extend TCS network layout and visualization. *Bioinformatics*, **32**, 627–628.

Schröder-Ritzrau, A., Freiwald, A. & Mangini, A. (2005) *U/Th-dating of deep-water corals from the eastern North Atlantic and the western Mediterranean Sea*. *Cold-Water Corals and Ecosystems* (ed. by A. Freiwald) and J.M. Roberts), pp. 157–172. Springer-Verlag Berlin Heidelberg.

Shum, P., Pampoulie, C., Kristj, A. & Mariani, S. (2015) Three-dimensional post-glacial expansion and diversification of an exploited oceanic fish. *Molecular Ecology*, **24**, 3652–3667.

Strömberg, S.M. & Larsson, A.I. (2017) Larval Behavior and Longevity in the Cold-Water Coral Lophelia pertusa Indicate Potential for Long Distance Dispersal. *Frontiers in Marine Science*, **4**, 32–33.

Stumpf, R., Frank, M., Schönfeld, J. & Haley, B.A. (2010) Late Quaternary variability of Mediterranean Outflow Water from radiogenic Nd and Pb isotopes. *Quaternary Science Reviews*, **29**, 2462–2472.

Tajima, F. (1983) Evolutionary relationship of DNA sequences in finite populations. *Genetics*, **105**, 437–460.

Taviani, M., Vertino, A., López Correa, M., Savini, A., de Mol, B., Remia, A., Montagna, P., Angeletti, L., Zibrowius, H., Alves, T., Salomidi, M., Ritt, B. & Henry, P. (2011) Pleistocene to Recent scleractinian deep-water corals and coral facies in the Eastern Mediterranean. *Facies*, **57**, 579–603.

Vertino, A., Stolarski, J., Bosellini, F.R. & Taviani, M. (2014) Mediterranean Corals Through Time: From Miocene to Present. *The Mediterranean Sea: Its History and Present Challenges*, 1–678.

Voelker, A.H.L., Lebreiro, S.M., Schönfeld, J., Cacho, I., Erlenkeuser, H. & Abrantes, F. (2006) Mediterranean outflow strengthening during northern hemisphere coolings: A salt source for the glacial Atlantic? *Earth and Planetary Science Letters*, **245**, 39–55.

Waller, R.G. & Tyler, P.A. (2005) The reproductive biology of two deep-water, reef-building scleractinians from the NE Atlantic Ocean. *Coral Reefs*, **24**, 514–522.

929 Wedding, L.M., Reiter, S.M., Smith, C.R., Gjerde, K.M., Kittinger, J.N., Friedlander, a. M., Gaines,
930   S.D., Clark, M.R., Thurnherr, a. M., Hardy, S.M. & Crowder, L.B. (2015) Managing mining of the
931   deep seabed. *Science*, **349**, 144–145.

932 Weinberg, C., Titschack, J., Freiwald, A., Frank, N., Lundälv, T,, Taviani, M., Beuck, L., Schröder-
933   Ritzrau,, A., Krengel, T. & Hebbeln, D. (2018) The giant Mauritanian cold-water coral mound
934   province: Oxygen control on coral mound formation. *Quaternary Science Reviews*,**185**,135-152.

935 Weir, B.S. & Cockerham, C.C. (1984) Estimating F-statistics for the analysis of population structure.
936   *Evolution*, **38**, 1358–1370.

937 White, M., Mohn, C., Stigter, H. de, & Mottram, G. (2005) Deep-water coral development as a function
938   of hydrodynamics and surface productivity around the submarine banks of the Rockall Trough,
939   NE Atlantic. *Cold-water Corals and Ecosystems* (ed. by A. Freiwald and J.M. Roberts), pp. 503–
940   514. Springer, Erlangen Earth Conference Series, Berlin, Heidelberg.

941 Widmer, A. & Lexer, C. (2001) Glacial refugia: Sanctuaries for allelic richness, but not for gene
942   diversity. *Trends in Ecology and Evolution*, **16**, 267–269.

943 Wilson, A.B. & Eigenmann Veraguth, I. (2010) The impact of Pleistocene glaciation across the range
944   of a widespread European coastal species. *Molecular Ecology*, **19**, 4535–4553.

945 Zahn, R., Schönfeld, J., Kudrass, H.R., Park, M.H., Erlenkeuser, H. & Grootes, P. (1997)
946   Thermohaline instability in the North Atlantic during melt water events: Stable isotope and ice-
947   rafted detritus records from core SO75-26KL, Portuguese margin. *Paleoceanography*, **12**, 696–
948   710.

949 Zibrowius, H. (1980) *Les Scléractiniaires de la Méditerranée et de l'Atlantique nord-oriental*, Institut
950   Oceanographique Fondation Albert 1er, Prince de Monaco.

951

952 xi. Biosketch

953 Ronan Becheler is a postdoctoral researcher in evolutionary ecology and population
954 genetics. His research interests concern the evolutionary consequences of reproductive
955 systems, with a special emphasis on partial clonality. He has worked on the assessment of
956 dispersal in coastal and deep-sea species. Currently, he studies the evolution of reproductive
957 strategies and local adaptation in temperate macroalgae.

958 Joana Boavida is a postdoctoral researcher interested in biodiversity-related disciplines, from
959 taxonomy to biogeography and macroecology, typically using corals as model systems.

960 xii. Appendices

961 The appendix shows supporting information

962 xiii. Supporting information is supplied in a separate file

963 Table S1 - Summary of sampling locations and associated information.

964 S2 - Additional methods.

965 Table S3 - Pairwise F_{ST} based on ITS haplotypic frequencies.

966 Table S4 - Pairwise F_{ST} for microsatellites.

967 Table S5 - Analysis of molecular variance (AMOVA) for microsatellites.